A Raman and XPS investigation of supported molybdenum oxide thin films. 2. Reactions with hydrogen sulfide

ARTICLE *in* CHEMINFORM · OCTOBER 1993

Impact Factor: 0.74 · DOI: 10.1021/j100144a021

2 AUTHORS, INCLUDING:

Norman S Mcintyre
The University of Western Ontario
232 PUBLICATIONS **6,344** CITATIONS

SEE PROFILE

A Raman and XPS Investigation of Supported Molybdenum Oxide Thin Films. 2. Reactions with Hydrogen Sulfide

Perry A. Spevack* and N. S. McIntyre

Surface Science Western, University of Western Ontario, Laurene O. Patterson Bldg, Western Science Centre, London, Ontario, Canada N6A 5B7

*Received: March 17, 1993; In Final Form: August 9, 1993**

Surface characterization of supported molybdenum oxide thin films is undertaken following sulfidation treatments with H_2S. Surface characterization is carried out by *in situ* and *ex situ* laser Raman spectroscopy (LRS) and X-ray photoelectron spectroscopy (XPS). Sulfidation of thin-film molybdenum oxides supported on planar alumina and graphite produces two sulfides species: MoS_2 and a reduced form with a binding energy lower than MoS_2. The S(2p) spectra also show polysulfide species at higher binding energies to MoS_2. Sulfidation of thicker, octahedral MoO_3 thin films results only in MoS_2. Extensive prereduction of octahedral MoO_2 prior to sulfidation is shown not to be important in the conversion of oxide to sulfide phases.

Introduction

Hydrodesulfurization (HDS) catalysts are used to remove sulfur from petroleum feedstocks before the feedstocks are treated over hydrocracking and other specialized catalysts. The HDS catalyst uses molybdenum oxide frequently promoted with cobalt or nickel oxides and supported on a high surface area catalyst such as γ-alumina, although some wor s has been focused on the viability of using TiO_2,[1] silica,[2,3] silica–alumina,[4–6] or carbon[7–11] as alternative supports. The catalyst is calcined and reduced and frequently presulfided to activate the material. If the catalyst is not presulfided prior to use, it becomes sulfided during use.[6] During the early studies on molybdenum-based HDS catalysts, it was discovered that the sulfided phase was responsible for the catalytic action.[6,12] In the 25 years of work that have followed this discovery, it has been accepted that the HDS-active site resides in a MoS_2-like environment for a fully sulfided catalyst.[6,10,12] While the exact nature of this MoS_2-like phase and the promoting effect that cobalt and nickel ions have on this phase remain as a contentious research issue, the mechanism of sulfur abstraction from organo-sulfur compounds appears to be in agreement among most research groups.[6,10,13–15]

The catalytic mechanism involves the adsorption of an organo-sulfur compound at a coordinatively unsaturated site in the MoS_2 lattice, specifically at a singly or doubly vacant anion location(s) which may be found at corner and edge positions on MoS_2 slabs. During adsorption, electrons are believed to be donated from a reduced molybdenum center (<Mo(IV)) to facilitate C–S bond scission.[6] Such a process would then oxidize the molybdenum back to a Mo(IV) state. The role of hydrogen in the reaction is to regenerate the adsorption site by forming H_2S with the newly adsorbed sulfur atom and thereby re-forming the reduced molybdenum center. Two possible roles that the promoter ions (i.e., Co and Ni) serve is to supply available surface hydrogen, probably in the form of SH^- groups, and to return the Mo(IV) ion to its initial, reduced state through electron transfer.[6]

The number of active sites present on the surface of a catalyst will depend on the abundance of suitable unsaturated centers such as the aforementioned corner and edge sites. These, in turn, will depend on the size of the S–Mo–S slabs of the MoS_2 lattice and the presence of defects which can mimic these sites. At these centers there is a disruption in the S–Mo–S framework yielding the unsaturated molybdenum centers. The reaction mechanism as stated above implies the presence of a molybdenum valence state less than IV at the unsaturated centers—perhaps Mo(III) or Mo(II). Some of the surrounding sulfur anions may possess dangling sulfur bonds. Few studies of the reduced Mo reaction site or the surrounding anions have been conducted, despite the obvious importance of these factors to the success of the HDS catalyst.

This laboratory has been using thin molybdenum oxide films to explore the oxide and sulfide species present during all stages in the preparation of supported molybdenum HDS catalysts.[16–19] This study serves as a companion paper to a study which examined aspects of calcination and reduction of supported and unsupported thin-film catalysts.[20] In the present paper we report XPS (X-ray photoelectron spectroscopy) and LRS (laser Raman spectroscopy) results of the sulfidation processes carried out on such films. The sulfidation products of thin supported molybdenum oxide films are identified and compared to those originating from a bulk, octahedral MoO_3 phase. The sulfidation efficiencies (completeness of sulfidation) of "reduced MoO_3" is compared to that of octahedral MoO_3. High-resolution XPS has identified a molybdenum species with a valence state <IV on sulfided thin films. Two or three sulfur species have been observed on the thin films in addition to the sulfide species normally associated with MoS_2. The possible link between these Mo(3d) and S(2p) species and the catalytic centers involved in HDS processes are discussed.

Experimental Section

Spectroscopic Analysis. XPS analysis is carried out on a modified SSL X-Probe spectrometer utilizing a monochromatized Al Kα X-ray source. Spectra are referenced either to an Al(2p) binding energy of 74.5 ± 0.1 eV for an amorphous alumina[21–23] or to the residual hydrocarbon contamination at 284.9 ± 0.1 eV. Angle-dependent XPS (ARXPS) spectra were taken at shallow and deep take-off angles, corresponding to mean sampling depths of 2 and 6 nm, respectively. A peak-fitting paradigm previously developed for the deconvolution of oxide species from Mo(3d) spectral envelopes has been extended to include sulfide compounds prepared during the course of this work and from earlier studies[17,24] (see Table I). Sulfur spectra are fitted with 90% Gaussian/10% Lorentzian peak shapes with spin–orbit intervals and ratios of 1.19 eV and 2.00 ± 0.05, respectively. Raman spectra were recorded on a Dilor Omars 89 spectrometer using the 476.49-nm line of an argon ion laser. Powdered MoO_3 (Alfa products) and natural molybdenite (Molly Hill mine) were used as reference materials and for calibration purposes (±5 cm^{-1}). Instrument specifications for XPS and LRS, quantification details, and Mo-(3d) spectral parameters may be found elsewhere.[17,20]

* Abstract published in *Advance ACS Abstracts*, October 1, 1993.

0022-3654/93/2097-11031$04.00/0

TABLE I: XPS Binding Energies for Molybdenum Compounds

	binding energy[a]				
compd	$MO(3d_{5/2})$	fwhm	O(1s)[b]	fwhm	ref
Mo(0)	227.8	0.56 (0.77)[c]			*f*
MoO_2	229.2	0.64 (0.74)[c]	529.9	1.1	*g*
Mo(IV)	230.1	1.35			*g*
Mo(V)	231.2	1.35			*g*
Mo(VI)[d]	232.7	1.55	530.9	1.3	*f, g*
MoO_3	232.7	1.0	530.6	1.3	*g*
			$S(2p_{3/2})$		
MOS_{2-x}			161.2	0.8	*f, h*
MoS_2[c]	229.0	0.94 (1.00)[c]	161.9	0.8	*f, h*
Mo(S–S)			162.6	0.8	*f, h*
Mo(S–S)			163.4	0.8	*f, h*

[a] BE = ±0.1 eV. [b] Main O(1s) peak. [c] $Mo(3d_{3/2})$ component in parentheses. [d] Nonoctahedral environment. [e] Sulfided thin film. [f] See ref 20. [g] See ref 16. [h] See refs 17, 18, 24, 40, and 41.

Film Preparation and Sulfidation Treatment. The precursor molybdenum oxide films prepared for this work are described elsewhere.[20] Thin films (<1–20 nm) were deposited on planar alumina or graphite. Thicker (>100 nm) films were grown on molybdenum metal. All sulfidation reactions were carried out in an *in situ* quartz reaction cell described elsewhere[20] or in a high-pressure, high-temperature stainless steel microreactor mated to the sample load lock of a SSL X-Probe ESCA spectrometer.[25] A 2% H_2S/H_2 gas mixture (Matheson) was used for sulfiding the samples. The gas flow was regulated at 50 mL min^{-1} through a stainless steel flowmeter. During the sulfidation procedure, all samples were subjected to a $^1/_2$-h prereduction in flowing H_2 at the reaction temperature (unless otherwise stated) immediately prior to introducing the sulfiding gas mixture. This prereduction was part of a methodology which has been used in previous studies.[18,25] Sulfidation reactions were carried out at 350 °C for periods of 30 min or longer (see text). Following sulfidation, the reactor was purged with high-purity argon (Matheson) during cool-down. All sample transfers following *in situ* reduction and/or sulfidation were carried out under an inert atmosphere of dry N_2 or Ar via a glovebag[26] to the XPS introduction chamber for further analysis.

Results

Sulfidation of Thin-Film Molybdenum Oxides. Thin films of planar alumina and graphite-supported molybdenum oxide were calcined to obtain a largely amorphous oxide.[20] The samples were then reduced and sulfided for $^1/_2$ h each at 350 °C and were transferred without exposure to air into the XPS for analysis. The XP spectra of some of a series of planar alumina- and graphite-supported samples are shown in Figures 1 and 2, respectively. Several $Mo(3d_{5/2})$ peaks could be fitted for each Mo(3d) envelope, indicating that more than one molybdenum species was present. In most of the spectra, the main molybdenum component was MoS_2, with a $Mo(3d_{5/2})$ binding energy of 229.0 eV.[17,18,24,27,28] Besides MoS_2, all samples contain three additional Mo(3d) peaks at binding energies of 230.0, 231.2, and 232.6 eV, corresponding to the oxides of Mo(IV), Mo(V), and Mo(VI), respectivey.[16,20] The assignment of the MoS_2 species should be qualified since its binding energy overlaps with that of MoO_2 (Table I). This makes identification of MoO_2 in the presence of MoS_2 difficult by use of the Mo(3d) spectra alone. S(2p)/Mo(3d) ratios obtained from survey scan analyses can be used to confirm the amount of MoS_2 present in the Mo(3d) spectra. Using a S/Mo = 2 for bulk MoS_2, one can calculate the amount of MOS_2 present on each surface. For example, the ~100 nm thick specimen in Figure 3 has a S(2p)/Mo(3d) ratio of 1.45, which corresponds to ~70% MoS_2. This calculated value is in close agreement with the tabulated results (presented in Figure 3) obtained from the peak-fitted data.

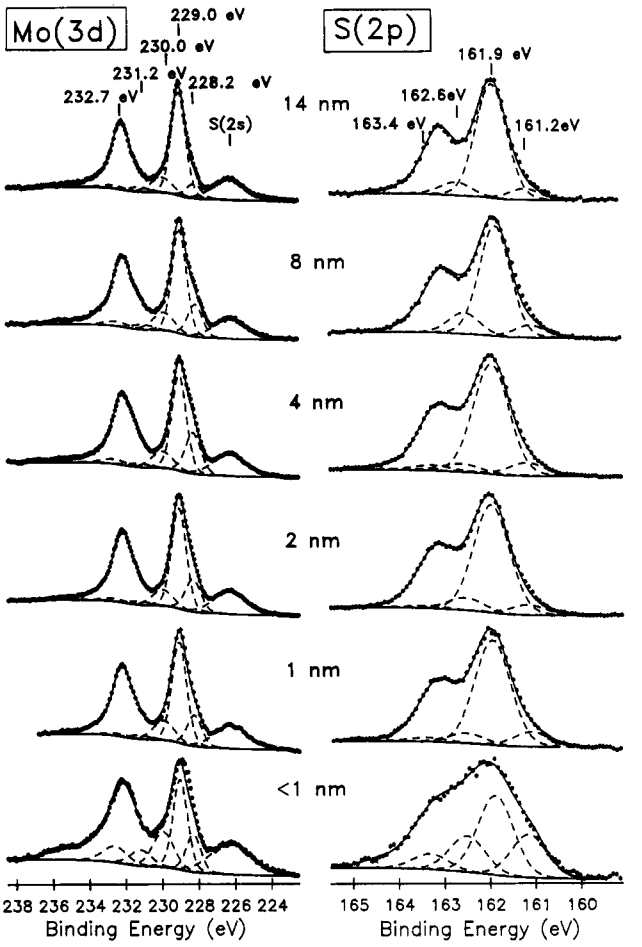

Figure 1. Mo(3d) and corresponding S(2p) XPS spectra of planar alumina-supported molybdenum oxide thin films following sulfidation at 350 °C in 2% H_2S/H_2 for $^1/_2$ h. Only $Mo(3d_{5/2})$ and $S(2p_{3/2})$ spin–orbit components have been shown for clarity.

At thicknesses less than ~20 nm, the alumina- and graphite-supported thin films show a contribution from a Mo(3d) peak at a BE = 228.2 eV. A Mo(3d) peak at a similar binding energy has been previously observed on ion-bombarded[24] and lithographically-textured[27] basal plane MoS_2 surfaces. It has been proposed to be a sulfur-depleted species or a "Mo defect" structure, respectively. Quantification reveals that all samples containing the $Mo(3d_{5/2})$ peak at 228.2 eV have an excess concentration of sulfide sulfur remaining after accounting for all the MoS_2. Furthermore, the S/Mo ratio for this species is ~1:1 for all of the samples analyzed. The binding energy of this species suggests an oxidation state less than IV (see Table I). Two literature references have identified a Mo(II) species at a binding energy of 228.2 eV on alumina- and TiO_2-supported catalysts.[29,30] This indicates that a possible stoichiometry for the compound may be MoS. While it is sometimes questionable to use oxide binding energies as references for sulfur analogues, the references in question are not used for absolute proof but rather for qualitative support of the sulfur analogue peak assignments. The S(2p) spectra for all of the sulfided thin films contain two or three sulfur components in addition to the major species, sulfide of MoS_2 at 161.9 eV: one of the additional species has a $S(2p_{3/2})$ binding energy of 161.2 eV, which we believe to be a S^{2-} component experiencing a different potential from MoS_2; the higher binding energy peaks at 162.6 and 163.4 eV may correspond to polysulfide or thiomolybdate species (i.e., Mo_xS_y, $x \neq y > 1$).

Representative Raman spectral data taken of some of the sulfided thin films (Figure 4) show the presence of some crystalline MoS_2 (peaks at 408 and 385 cm^{-1})[5,31–35] atop an amorphous background. Some structure at ~100–250 cm^{-1}, has been observed by others on sulfided catalyst samples,[31,33] but no evidence

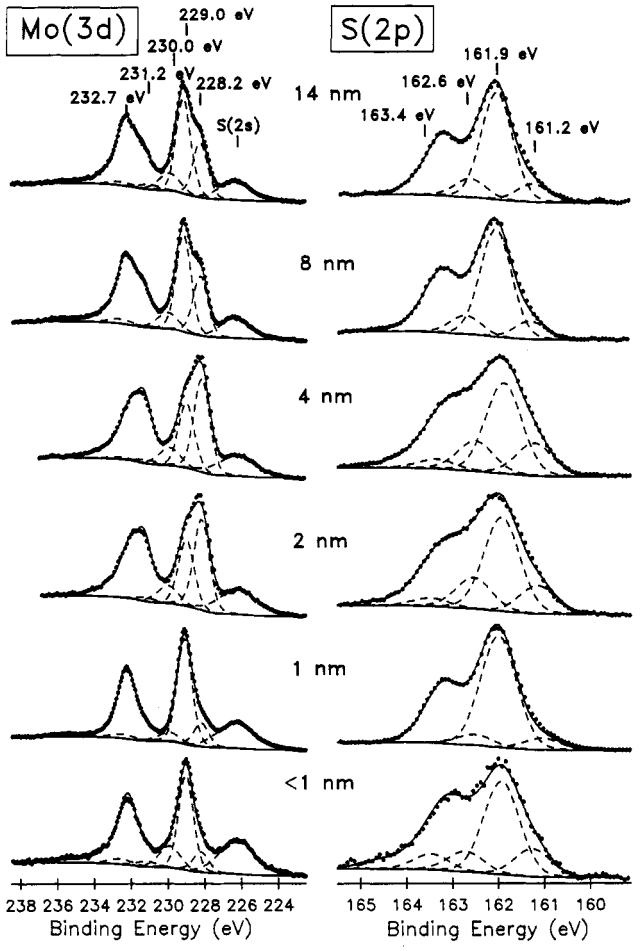

Figure 2. Mo(3d) and corresponding S(2p) XPS spectra of graphite-supported molybdenum oxide thin films following sulfidation at 350 °C in 2% H_2S/H_2 for $^1/_2$ h. Only Mo($3d_{5/2}$) and S($2p_{3/2}$) spin–orbit components have been shown for clarity.

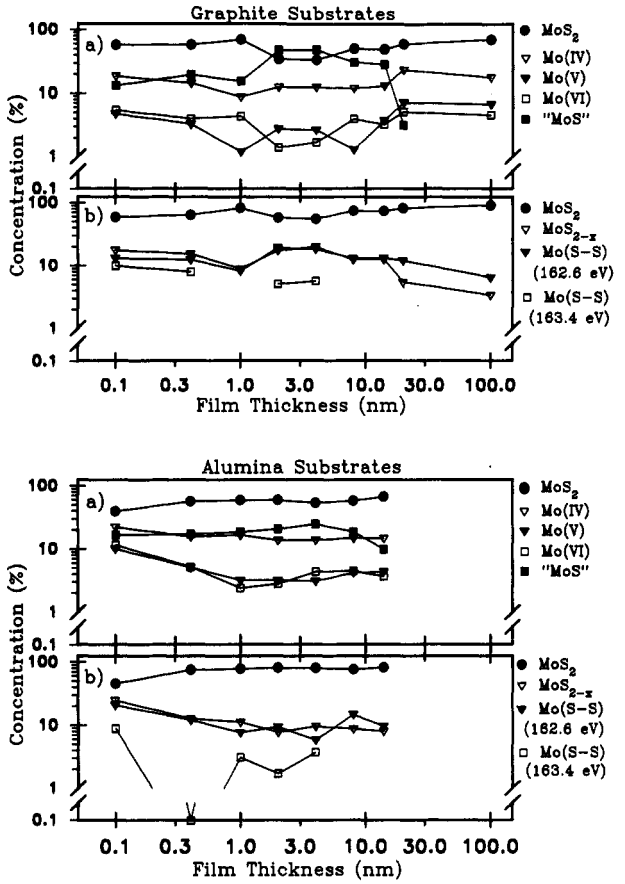

Figure 3. Concentration of Mo(3d) and S(2p) curve-fitted components for graphite-supported and planar alumina-supported molybdenum thin films following sulfidation at 350 °C in 2% H_2S/H_2 for $^1/_2$ h: (a) Mo(3d) data, (b) S(2p) data. Note: the 100-nm film is supported on molybdenum metal.

of additional sulfur species is present. In particular, there is no Raman evidence of a sulfur species which may correspond to the peaks observed by XPS for the reduced molybdenum species at BE = 228.2 eV.

II. Sulfidation of Crystalline MoO_3 vs "Reduced MoO_3". The sulfidation efficiencies of reduced molybdenum trioxide (see below) and crystalline MoO_3 thin film specimens were compared. Two thick (>100-nm) films of crystalline MoO_3 were grown on Mo(0) substrates.[20] In this test, one sample, "sample A", was reduced in H_2 at 500 °C for >12 h and then treated with aqueous ammonia prior to sulfidation at 350 °C for $^1/_2$ h. The aqueous ammonia treatment was intended to ensure that no octahedral MoO_3 remained on the sample prior to sulfidation.[20] A second sample, "sample B", was reduced in H_2 at 350 °C for 1/2 h followed by sulfidation for $^1/_2$ h under the same conditions. This $^1/_2$-h reduction treatment at 350 °C, a standard catalyst pretreatment used in previous work,[18,25] has been shown to yield a small amount of Mo(V) in the presence of Mo(VI) according to the Mo(3d) XP spectrum.[16] The Mo(3d) spectra of each sample prior to sulfidation and the Mo(3d) and S(2p) spectra following sulfidation are shown in Figure 5. The spectra show little difference between the number and type of peaks present following sulfidation of the two samples. ARXPS results (not shown) taken at sampling depths of ~6 and 2 nm illustrate both the uniformity in composition for each sample following the sulfidation procedure and the similarity in composition between the two samples. The conditions chosen for sulfidation do not differentiate between octahedral MoO_3 and "reduced MoO_3" and appear to result in equal sulfidation of both samples. In contrast with the thinner (≤20 nm) samples, the thick specimens (>100 nm) do not show evidence of the reduced Mo(3d) peak at BE = 228.2 eV.

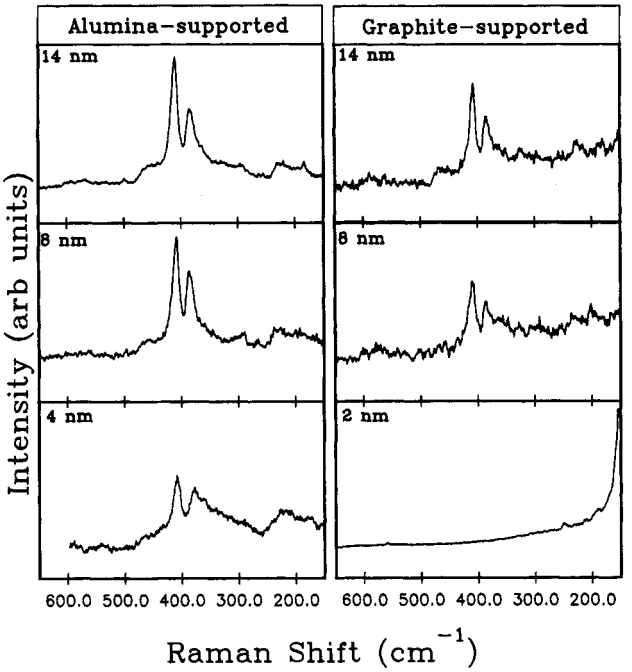

Figure 4. Representative Raman spectra of sulfided alumina- and graphite-supported thin films (2% H_2S/H_2 at 350 °C for $^1/_2$ h). Corresponding XPS spectra are shown in Figures 1 and 2.

Sulfidation for different times from $^1/_2$ to 2 h was used to determine whether a complete conversion of oxide into bulk MoS_2 could occur. No significant differences in XPS Mo(3d) or S(2p) spectra could be found. A similar experiment was conducted on a sample of octahedral MoO_3 decomposed by heating *in vacuo*

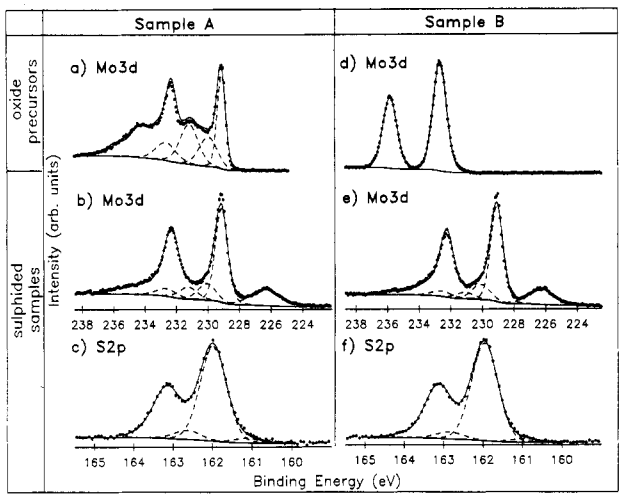

Figure 5. XPS Mo(3d) and S(2p) narrow scan spectra following sulfidation treatments on two molybdenum-supported oxide samples: (a) sample A prereduced in H_2 at 500 °C for >12 h; (b) sample A sulfided in 2% H_2S/H_2 at 350 °C for $^1/_2$ h; (c) S(2p) spectrum of sample A; (d) sample B, octahedral MoO_3 precursor; (e) sample B reduced and sulfided for $^1/_2$ h at 350 °C in H_2 and 2% H_2S/H_2, respectively; (f) S(2p) spectrum of sample B. Only Mo($3d_{5/2}$) and S($2p_{3/2}$) spin–orbit components are shown for clarity; S(2s) peaks are shown in (b) and (e). See Table I for peak identities.

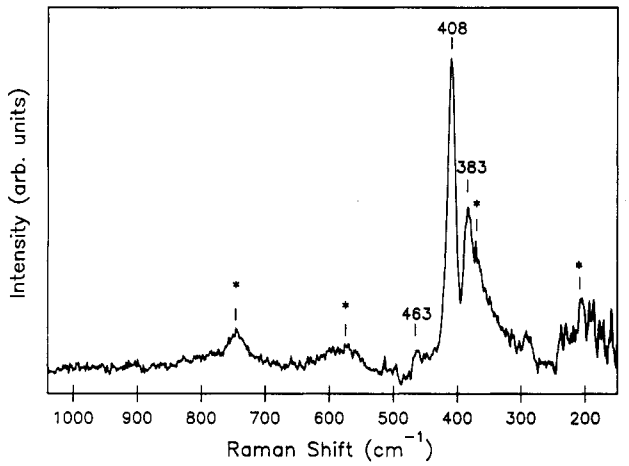

Figure 6. *In situ* Raman spectra of octahedral MoO_3/Mo reduced *in vacuo* for 13 h at 500 °C and sulfided at 350 °C in 2% H_2S/H_2 for $2^1/_2$-h total sulfidation time. Asterisk denotes spectral peaks due to MoO_2.

for 13 h at 500 °C and then sulfided for $2^1/_2$ h in flowing 2% H_2S/H_2 at 350 °C. The *in vacuo* heating procedure has been shown to result in a reduced molybdenum phase which is equivalent to that shown in Figure 5a.[20] *In situ* Raman results (not shown) of the sulfided film reveals that a small amount of MoO_2 remains on the surface after 1-h sulfidation. Lengthening the treatment time to $2^1/_2$ h (Figure 6) did not effect any substantial changes in the spectral composition. Our LRS calibration indicate that the scattering cross section of MoS_2 is ~2–4 times lower than for MoO_2; this suggests that the concentration of MoO_2 found in the LRS spectra is small in comparison to the MoS_2. These results indicate that our XPS peak-fitting assumption for the sulfided films is not entirely correct since some MoO_2 remains on the sulfided surfaces, but the assumption is still reasonable since the concentration of MoO_2 left on the sample is small compared to the MoS_2.

The major Mo(3d) sulfur species which results from the sulfidation of thick films (>100 nm) of octahedral MoO_3 or "reduced MoO_3" is MoS_2. The XPS narrow scan spectra and the quantitative data from the survey scans corroborate this finding. In the S(2p) spectra, the sulfide, S^{2-}, corresponding to MoS_2, is the major sulfur species present. S/Mo ratios for thick (>100 nm) sulfided molybdenum oxide films can be adequately explained on the basis of a single sulfide species.

Discussion

Sulfidation of Thin-Film Molybdenum Oxides. The concentration of the individual molybdenum species appears to be fairly constant over the range of thicknesses studied on the alumina substrates as evident from Figures 1 and 3, with the exception of the thinnest films. Films <1 nm tend to have higher concentrations of Mo(VI), -(V), and -(IV) oxides and somewhat lower concentrations of MoS_2. This reflects a more stable molybdate surface species which is bonding directly with the alumina substrate. Furthermore, replacement of Al–O–Mo oxygen species with sulfur is likely to be more difficult because of steric considerations and would likely require higher temperatures and prolonged sulfiding times than those used in this work.[36]

All of the samples contain additional sulfur species besides sulfide in MoS_2. One of the components appears at a lower binding energy than S^{2-} in MoS_2, and two components occur at higher binding energies. The shape of the S(2p) envelope is quite similar over all of the thicknesses reported in Figure 1, with the exception of the thinnest specimen (<1 nm). This trend is also reflected in the data presented in Figure 3. The thinnest films have substantially higher concentrations of the lower and higher binding energy components. As was noted above, the thinnest films have a higher concentration of the Mo(VI)/(IV) oxides. The lower and higher binding energy sulfur species are not likely to be associated with these oxide species. The formation of any oxysulfide species would produce spectral peaks at ~167–170 eV, the region where S–O bonding is present.[17,37,38] However, it is possible that a molybdenum sulfide species may overlap with the spectral peaks previously assigned to the oxide species. This point will be discussed below.

The sub-sulfide component (161.2 eV) has been designated as a S^{2-} species experiencing an electronic potential higher than that of sulfur in MoS_2. A similar peak has been reported on ion-dosed MoS_2 basal plane surfaces[24] and on a fractured pyrrhotite surface.[39] The two additional peaks found at higher binding energies to the S^{2-} peak have been ascribed to polysulfide or thiomolybdate species. Polysulfides of molybdenum are well-known, with disulfide ligands, S_2^{2-}, being the most prevalent.[40,41] They have been observed on single-crystal MoS_2 following neon ion bombardment.[40] The disulfide linkage may form as a result of two dangling sulfur atoms combining through an oxidation reaction.[40] The peak at 163.4 eV may also be due to a disulfide linkage, albeit one in a slightly different electronic environment from the peak at 162.6 eV. Both spectral peaks fall near the range of binding energies reported for molybdenum polysulfides with disulfide ligands: ~162.9–164.3 eV.[42,43] Although less probable, the higher binding energy peak may be associated with a longer polysulfide chain, such as a trisulfide ligand. As the polysulfide chain increases, the sulfur atom furthest removed from the metal atom will experience a binding energy less like that of S^{2-} (BE = 161.9 eV) and more like that of amorphous sulfur, S_8 (BE ~164 eV).[37,38] A coordinatively unsaturated center with an anion vacancy (or a pair of anion vacancies) would present a suitable environment for the formation of a disulfide ligand.

Alternatively, the higher binding energy S(2p) peaks may be due to thiomolybdate species, which have a core structure of Mo_xS_y, where $x \neq y > 1$. Such structures are also well-known in molybdenum chemistry[41] and possess S(2p) binding energies in the range 162.3–163.2 eV. Thiomolybdate formation may also be associated with defect sites (anion vacancies) in the MoS_2 lattice where S/Mo ratios are near unity. The polysulfide and thiomolybdate structures should not be considered as mutually exclusive, since a thiomolybdate species may contain one or more disulfide ligands. Mo(3d) binding energies for some of these thiolates occur at binding energies of 228.0–230.4 eV[41,42,44] for molybdenum valences of (III)–(VI). This falls in the range of positions occupied by MoS_2 and Mo(IV) oxide. Given the relatively low concentrations of these sulfur species and the complex nature of the Mo(3d) spectral envelope, it would be

mere conjecture to assign a Mo(3d) spectral peak(s) to one or more of these structures without corroborating evidence from another soure. There is substantial Raman documentation on these thiolate species.[31,35,41,43,44] Spectral peaks for these thiolates occur as follows: ν(Mo–S) ~ 310–380 cm^{-1}, ν(Mo–Mo) ~ 160–260 cm^{-1}, and ν(S–S) ~ 510–560 cm^{-1}. No Raman evidence of any polysulfide or thiomolybdate species has been found on the spectra shown in Figure 4 or in any other spectra accumulated during the course of this work. Again, this maybe due to the small concentration of thiolates involved; this is further complicated by the unknown scattering cross section for these thiolate species compared to the strongly scattering MoS_2 present on these samples.

The concentrations of the individual molybdenum species on the graphite-supported thin films vary considerably more than on the alumina-supported samples. The most obvious difference lies in the concentrations of the MoS_2 and the 228.2-eV peak assigned as a reduced molybdenum sulfur species. Over the thickness range 2–14 nm, the concentration of the 228.2-eV peak is considerably higher than in the alumina-supported samples. There would appear to be a range of thicknesses over which the concentration of the 228.2-eV peak increases and then decreases. Film thicknesses greater than ~20 nm supported on graphite do not show the presence of this reduced sulfur peak (Figure 3), nor do sulfided thick (>100 nm) films grown on molybdenum metal (Figure 5).

In the companion study on the behavior of the calcined thin film precursors,[20] it was suggested that the sputter deposition process used to prepare the supported thin films produces oxide clusters of varying size with a low-ordered structure which may be termed "amorphous". The presence of the reduced sulfur species may be associated with this "amorphous" structure. At thicknesses above ~20 nm where XPS and Raman spectra of the calcined precursors show only octahedral MoO_2 present,[20] the sulfided films no longer show the presence of the reduced sulfur species. The amorphous clusters may facilitate the further reduction of the oxide samples beyond the MoS_2 phase to produce a small concentration of the reduced sulfide phase (228.2-eV peak). It is not known why thicknesses of ~2–4 nm on graphite substrates produce the highest concentrations of this peak. This range of thicknesses may yield an "ideal" cluster size which reduces more completely. It is also difficult to explain the differences between the alumina- and graphite-supported films with regard to the concentration of the reduced sulfur species. In the range of film thicknesses involved, there is no "support interaction" of the type normally associated with Mo/Al_2O_3. Possibly, the different support reactivities can influence the size of the clusters, and this, in turn, has an effect on the likelihood of formation of the reduced sulfide peak (BE = 228.2 eV).

The reduced Mo(3d) sulfide peak may be associated with the active site on the sulfided surface of the HDS catalyst. It is reasonable to suggest that the reduced sulfide species may be present in and related to the MoS_2 lattice in the sulfided thin films. The reduced sulfide species may be a thiomolybdate as discussed above. A core thiomolybdate structure, Mo_3S_4, has been obtained through cyanolysis of the mineral jordisite (noncrystalline MoS_2).[44] Müller has also shown schematically how a thiolate containing disulfide linkages, $[Mo_3S(S_2)_6]^{2-}$, can transform into an extended MoS_2 lattice through the removal of S atoms during heating.[45] Furthermore, the presence of similar Mo(3d) species found on ion-sputtered MoS_2 single-crystal surfaces by a number of groups[24,27,40] and the occurrence of similar accompanying S(2p) species lends support to the assignment of this peak as being due to a MoS-type species. Additionally, the fact that this spectral peak was observed on both alumina and graphite supports would seem to negate the possibility of this peak being due to some Mo–C interaction, as has been suggested recently by Bouwens et al.[9]

Despite the substantial concentrations of the reduced Mo(3d) sulfide peak (especially in some of the graphite-supported thin films), there has not been any definitive Raman spectrum observed which can be associated with this species. It is quite possible that this species is not Raman active, and therefore no spectrum should be present. However, if one postulates that this species *is* Raman active, than we must consider possible reasons why a Raman spectrum has not been observed. As was suggested earlier, the very intense Raman scattering of MoS_2 may swamp the signal of this MoS-like species. If this MoS species represents a defect in the MoS_2 lattice which results largely from the removal of S atoms in the Mo backbone, then it seems unlikely that any substantial change in the Mo–S Raman frequencies of MoS_2 should be observed. Furthermore, such a defect structure would probably be an amorphous phase rather than a discrete crystalline structure, which would result in a Raman spectrum containing broad peaks which could be more difficult to identify. The amorphous envelopes that lie beneath the MoS_2 peaks in Figure 4 (particularly in the 4-nm (alumina-) and 8-nm (graphite-) supported films) may be attributed to this defect molybdenum–sulfur species.

As discussed earlier, most researchers have acknowledged that a reduced molybdenum species of valence state II or III is necessarily involved during the catalytic HDS reaction. An Mo(III) center may be formed at a MoS_2 edge plane by the removal of sulfur ions by hydrogen involved in the catalytic reaction.[46,47] This species is necessary in the reductive pathway involved in the hydrogenolysis (S abstraction) of the organo-sulfur compound.[6] The molybdenum ion is oxidized in the process and must be regenerated by incoming H_2 or through electron donation by neighboring cobalt ions.[6,46] ESR studies have provided support for the existence of an Mo(III) state.[48,49] Previous work on sulfided Co–Mo–Al_2O_3 thin films has identified a Mo(3d) species at BE = 228.4 eV, which has been associated with specimens displaying hydrodesulfurization activity toward thiophene at temperatures of 275–350 °C and pressures of 0.1–0.3 MPa.[18,19] This subsulfide structure was postulated to be related to the "CoMoS" phase identified by Topsøe and co-workers.[50,51]

Sulfidation of Crystalline MoO_3 vs "Reduced MoO_3". Sulfidation experiments carried out on octahedral MoO_3 and a reduced specimen (reduced in H_2 at 500 °C for at least 12 h)[20] have shown that prereduction into primarily Mo(IV) oxide species prior to sulfidation has little effect on the efficiency of conversion into MoS_2. However, reduction using H_2/2% H_2S is much faster than using N_2 (or H_2) alone at 350 °C. In an earlier study,[16] no spectral evidence of molybdenum(IV) states was found after 1-h reduction of octahedral MoO_3 at 350 °C in N_2. In the present work, ~89% Mo(IV) (i.e., MoS_2 + Mo(IV)) was obtained after $^1/_2$ h of flowing H_2 followed by $^1/_2$ h of flowing 2% H_2S/H_2 carried out at 350 °C. This result is in agreement with results reported by Delmon's group,[52] which showed that reduction in H_2/H_2S occurs more rapidly than in dry H_2 alone. They said that the formation of MoO_2 hindered sulfidation into MoS_2, with sulfidation resulting in a mixture of MoO_2 and MoS_2. The present data do not show that the MoO_2 hinders the formation of MoS_2, but it is clear from the *in situ* Raman results in Figure 6 that some MoO_2 persists on the prereduced sample following sulfidation at 350 °C. According to Figure 3, XPS analysis reveals incomplete sulfidation to bulk MoS_2 on all sulfided samples. Increased sulfidation time (from $^1/_2$ to 2 h) gave no apparent increase in the concentration of MoS_2. Interestingly, both samples, "A" and "B", yielded similar concentrations of the intermediate Mo(IV)–Mo(VI) oxide species following sulfidation, despite the vastly different starting compositions.

The sulfidation mechanism of the prereduced and crystalline MoO_3 specimens may be explained by considering the crystallographic shear (CS) processes which were proposed for the reduction of crystalline MoO_3 (see companion paper, part 1). This CS mechanism involves the removal of anionic vacancies, such as point defects and screw dislocations, from the MoO_3 lattice through the formation of shear planes, which alter the lattice from corner-sharing to edge-sharing octahedra.[20] If we

first consider a prereduced sample that contains a substantial number of shear planes, the following processes are conceivable during sulfidation. The shear planes should be considered as facile pathways for diffusion of sulfur because they represent lines of high lattice energy between two stable, but mismatched, phases, namely, corner-sharing and edge-sharing molybdenum octahedra. Therefore, sulfur should be readily transported into the interior of the lattice through these shear planes, as well as through lattice defects. Once the sulfur has diffused into the lattice, four possible processes could occur. A sulfur atom (or ion) could exchange directly with an oxygen atom, or it could enter a lattice site vacated by an oxygen atom during reduction (anionic vacancy), or the sulfur could insert into a Mo–Mo bond (in MoO_2), or the sulfur atom could simply diffuse back out of the lattice. The fourth process does not add any sulfur to the material so we will ignore it in this discussion. The first and second processes involving direct sulfur–oxygen exchange and anion vacancy filling by sulfur, respectively, are the most favorable. The first process requires that a Mo(VI)–sulfur intermediate is formed, which is then immediately reduced to the 4+ state. The second process may be somewhat less likely to occur than the first process if the inserting species is a sulfur anion (rather than a neutral S atom) and the vacancy has trapped an electron (as molybdenum shear structures are known to do), since anion–electron repulsion will occur. The third process would be the least likely to occur since much higher energies would be required for sulfur to break the multiple Mo–Mo bonds in MoO_2 (see part 1, companion paper), compared to the energies required for sulfur insertion. This may explain why prereduction is usually avoided prior to sulfidation. It has been suggested that prereduction forms MoO_2 which is more difficult to sulfide.[52] While our data do not confirm that MoO_2 is necessarily more difficult to sulfide, the spectrum in Figure 6 does indicate that prereduced specimens contain small amounts of MoO_2 even after 2 h of sulfidation.

In the second case, if we consider a sample of crystalline MoO_3 which is reduced for $^1/_2$ h (essentially nonreduced) followed by $^1/_2$-h sulfidation, we can envisage the lattice as containing a small number of lattice defects (but no shear planes). Sulfur should be able to readily diffuse through these point defects into the lattice. Once inside the lattice, the same sulfur insertion processes can occur as in the prereduced sample. However, since sulfur insertion should occur concurrently with oxygen removal (reduction), the number of point defects present at a given time should be less than in the prereduced case, and therefore, crystallographic shear processes (and MoO_2 formation) should be less likely to occur. Therefore, a higher degree of sulfidation should be achieved than in the prereduced case.

Conclusions

1. A reduced molybdenum sulfur species with a binding energy of 228.2 eV has been observed on thin (<20-nm) supported oxide films following sulfidation at 350 °C. Graphite-supported samples show a higher concentration of this MoS species and a lower concentration of MoS_2 than do their equivalent planar alumina-supported films.

2. S/Mo ratios for thick (>100-nm) sulfided molybdenum oxide thin film species can be adequately explained on the basis of a single sulfide species. Spectral evidence shows no significant differences in the number or type of species resulting from the sulfidation of octahedral MoO_3 versus "reduced MoO_3".

References and Notes

(1) Ng, K. Y. S.; Gulari, E. *J. Catal.* **1985**, *92*, 340.

(2) Cheng, C. P.; Schrader, G. L. *J. Catal.* **1979**, *60*, 276.

(3) de Beer, V. H. J.; van der Aalst, M. J. M.; Machiels, C. J.; Schuit, G. C. A. *J. Catal.* **1976**, *43*, 78.

(4) Ahuja, S. P.; Derrien, M. L.; LePage, J. F. *Ind. Eng. Chem. Prod. Res. Dev.* **1970**, *9*, 272.

(5) Brown, F. R.; Makovsky, L. E.; Rhee, K. H. *J. Catal.* **1977**, *50*, 385.

(6) Gates, B. C.; Katzer, J. R.; Schuit, G. C. A. In *Chemistry of Catalytic Processes*; Ciofalo, R., Marshall, J., Leap, B., Eds.; McGraw-Hill: New York, 1979; Chapter 5, p 390.

(7) Groot, C. K.; de Beer, V. H. J.; Prins, R.; Stolarski, M.; Niedzwiedz, W. S. *Ind. Eng. Chem. Prod. Res. Dev.* **1986**, *25*, 522.

(8) Duchet, J. C.; van Oers, E. M.; de Beer, V. H. J.; Prins, R. *J. Catal.* **1983**, *80*, 386.

(9) Bouwens, S. M. A. M.; Prins, R.; de Beer, V. H. J.; Koningsberger, D. C. *J. Phys. Chem.* **1990**, *94*, 3711.

(10) Topsøe, H.; Clausen, B. S.; Topsøe, N.-Y.; Pedersen, E. *Ind. Eng. Chem. Fundam.* **1986**, *25*, 25.

(11) Daly, F. P.; Brinen, J. S.; Schmitt, J. L. *Appl. Catal.* **1984**, *11*, 161.

(12) Delmon, B. *Surf. Interface Anal.* **1986**, *9*, 195.

(13) Massoth, F. E. *Adv. Catal.* **1978**, *27*, 265.

(14) Hercules, D. M.; Klein, J. C. In *Electron Spectroscopy for Chemical Analysis Applied to Heterogeneous Catalysis*; Windawi, H., Ho, F. F.-L., Eds.; John Wiley and Sons: New York, 1982; Vol. 63, p 147.

(15) Ratnasamy, P.; Sivasanker, S. *Catal. Rev.—Sci. Eng.* **1980**, *22* (3), 401.

(16) Spevack, P. A.; McIntyre, N. S. *J. Phys. Chem.* **1992**, *96*, 9029.

(17) Spevack, P. A.; McIntyre, S. *Appl. Catal.* **1990**, *64*, 191.

(18) McIntyre, N. S.; Chan, T. S.; Spevack, P. A.; Brown, J. R. In Hydrotreating Catalysts: Preparation, Characterization and Performance. *Studies in Surface Science and Catalysis*; Occelli, M., Anthony, R., Eds.; Elsevier: Amsterdam, 1989; Vol. 50, p 187.

(19) McIntyre, N. S.; Chan, T. C.; Spevack, P. A.; Brown, J. R. *Appl. Catal.* **1990**, *63*, 391.

(20) Spevack, P. A.; McIntyre, N. S. *J. Phys. Chem.*, preceding paper in this issue.

(21) Cocke, D. L.; Johnson, E. D.; Merrill, R. P. *Catal. Rev.—Sci. Eng.* **1984**, *26* (2), 163.

(22) Halverson, D. E.; Cocke, D. L. *J. Vac. Sci. Technol.* **1989**, *A7* (1), 40.

(23) Fritsch, A.; Légaré, P. *Surf. Sci.* **1987**, *186*, 247.

(24) McIntyre, N. S.; Spevack, P. A.; Beamson, G.; Briggs, D. *Surf. Sci. Lett.* **1990**, *237*, L390.

(25) Spevack, P. A.; Coatsworth, L. L.; McIntyre, N. S.; Schmidt, I.; Brown, J. R. In Hydrotreating Catalysts: Preparation, Characterization and Performance. *Studies in Surface Science and Catalysis*; Occelli, M., Anthony, R., Eds.; Elsevier: Amsterdam, 1989; Vol. 50, p 229.

(26) Glovebag is a trademark of the "Instruments for Research and Industry, Inc." (I^2R); P.O. Box 159, Cheltenham, PA 19012.

(27) Roxlo, C. B.; Deckman, H. W.; Gland, J.; Cameron, S. D.; Chianelli, R. R. *Science* **1987**, *235*, 1629.

(28) Shuxian, Z.; Hall, W. K.; Ertl, G.; Knözinger, H. *J. Catal.* **1986**, *100*, 167.

(29) Quincy, R. B.; Houalla, M.; Proctor, A.; Hercules, D. H. *J. Phys. Chem.* **1990**, *94*, 1520.

(30) Yamada, M.; Yasumaru, J.; Houalla, M.; Hercules, D. M. *J. Phys. Chem.* **1991**, *95*, 7037.

(31) Schrader, G. L.; Cheng, C. P. *J. Catal.* **1983**, *80*, 369.

(32) Bartlett, J. R.; Cooney, R. P. In *Spectroscopy of Inorganic-based Materials*; Clark, R. J. H., Hester, R. E., Eds.; John Wiley and Sons: New York, 1987; p 187.

(33) Payen, E.; Kasztelan, S.; Houssenbay, S.; Szymanski, R.; Grimblot, J. *J. Phys. Chem.* **1989**, *93*, 6501.

(34) Chen, J. M.; Wang, C. S. *Solid State Commun.* **1974**, *14*, 857.

(35) Chang, C. H.; Chan, S. S. *J. Catal.* **1981**, *72*, 139.

(36) Massoth, F. E. *J. Catal.* **1975**, *36*, 164.

(37) Wagner, C. D.; Riggs, W. M.; Davis, L. E.; Moulder, J. F. In *Handbook of X-ray Photoelectron Spectroscopy*; Muilenberg, G. E., Ed.; Perkin-Elmer, Physical Electronics Division: Eden Prairie, MN, 1979; p 56.

(38) *NIST X-ray Photoelectron Spectroscopy Database*, Version 1.0; Wagner, C. D., Bickham, D. M., Eds.; National Institute of Standards and Technology: Gaithersburg, MD, 1989.

(39) *Developments in Mineral Processing, 6, Flotation of Sulfide Minerals*; Forssberg, K. S. E., Ed.; Elsevier: New York, 1985; p 41.

(40) Lince, J. R.; Stewart, T. B.; Hills, M. M.; Fleischauer, P. D.; Yarmoff, J. A.; Taleb-Ibrahimi, A. *Surf. Sci.* **1989**, *210*, 387.

(41) Müller, A.; Jostes, R.; Jaegermann, W.; Bhattacharyya, R. G. *Inorg. Chim. Acta* **1980**, *41*, 259.

(42) Müller, A.; Eltzner, W.; Jostes, R.; Bögge, H.; Diemann, E.; Schimanski, J.; Leuken, H. *Angew. Chem., Int. Ed. Engl.* **1984**, *23*, 389.

(43) Müller, A.; Diemann, E. In *Advances in Inorganic Chemistry*; Emelélus, H. J., Sharpe, A. G., Eds.; Academic Press: New York, 1987; Vol. 31, p 89.

(44) Müller, A.; Jostes, R.; Eltzner, W.; Nie, C.-S.; Diemann, E.; Bögge, H.; Zimmermann, M.; Dartmann, M.; Reinsch-Vogell, U.; Che, S.; Cyvin, S. J.; Cyvin, B. N. *Inorg. Chem.* **1985**, *24*, 2872.

(45) Müller, A. *Photohedron* **1986**, *5*, 323.

(46) Topsøe, H.; Clausen, B. S.; Candia, R.; Wivel, C.; Mørup, S. *J. Catal.* **1981**, *68*, 433.

(47) Ratnasamy, P.; Fripiat, J. J. *Trans. Faraday Soc.* **1970**, *66*, 2897.

(48) Voorhoeve, R. J. H. *J. Catal.* **1971**, *23*, 236.

(49) Konings, A. J. A.; van Dooren, A. M.; Koningsberger, V. H. J.; de Beer, V. H. J.; Farragher, A. L.; Schuit, G. C. A. *J. Catal.* **1978**, *59*, 1.

(50) Topsøe H.; Clausen, B. S.; Candia, R.; Wivel, R.; Morup, S. *J. Catal.* **1981**, *68*, 433.

(51) Wivel, C.; Candia, R.; Clausen, B. S.; Morup, S.; Topsøe, H. *J. Catal.* **1981**, *68*, 453.

(52) Grange, P. *Catal. Rev.—Sci. Eng.* **1980**, *21* (1), 135.